J Appl Electrochem (2010) 40:99–107
DOI 10.1007/s10800-009-9985-0

ORIGINAL PAPER

A voltammetric study on the corrosion of prestressed steel in saturated $Ca(OH)_2$ solution containing chloride ions

T. Henriques · A. Reguengos · L. Proença · E. V. Pereira · M. M. Rocha · M. M. M. Neto · I. T. E. Fonseca

Received: 4 March 2009 / Accepted: 16 August 2009 / Published online: 2 September 2009

Abstract An electrochemical study of prestressed steel in saturated $Ca(OH)_2$ aqueous solutions (pH 12) was carried out in the absence and in the presence of chloride ions, in such a concentration that simulates the composition of seawater. Cyclic voltammetry, linear sweep voltammetry, open circuit potential transients, atomic absorption spectroscopy and scanning electron microscopy coupled to electron diffraction spectroscopy were employed. The linear polarisation curves analysis led to the determination of polarisation resistance, R_p, corrosion potential, E_{corr}, corrosion current density, j_{corr}, Tafel slopes, breakdown potential, E_b and repassivation potential E_{repass}. A linear dependence of the breakdown potential, E_b, on the square root of scan rate was obtained, according to the Point Defect Model (PDM). A crossover characteristic of the nucleation processes was observed in the presence of chloride ions. SEM/EDS studies revealed, as expected, a strong influence of the presence of chloride ions observed in the transpassive and the active regions. In conclusion, chloride ions contribute to enhance the corrosion of steel, most probably due to their adsorption on both the active and the passive electrode surfaces.

Keywords Prestressed steel · Electrochemical studies · Chloride ions · Saturated $Ca(OH)_2$ solutions

T. Henriques · A. Reguengos · L. Proença · M. M. Rocha · M. M. M. Neto · I. T. E. Fonseca (✉)
Centro de Ciências Moleculares e Materiais (CCMM), Departamento de Química e Bioquímica, Faculdade de Ciências da Universidade de Lisboa, Campo Grande, Ed. C8, 1749-016 Lisbon, Portugal
e-mail: itfonseca@fc.ul.pt

L. Proença
Instituto Superior de Ciências da Saúde Egas Moniz, Quinta da Granja, Monte de Caparica, 2829-511 Caparica, Portugal

E. V. Pereira
Laboratório Nacional de Engenharia Civil (LNEC), Avenida do Brasil 101, Lisbon, Portugal

M. M. M. Neto
Departamento de Química Agrícola e Ambiental, Instituto Superior de Agronomia, TU Lisbon, Tapada da Ajuda, 1349-017 Lisbon, Portugal

1 Introduction

The prestressed steel has been used all over the world in large constructions (e.g. bridges, buildings, highways and pipelines), since its adoption in the mid 20s. Owing to economic and safety reasons, a careful survey is required in order to prevent corrosion problems [1–7]. The corrosion of prestressed steel in concrete has become a major technological problem. It is well known that many factors may influence the stability of steel passivity [2, 4, 7] in concrete. Accidental contamination by chloride ions may occur due to water, cement aggregates or exposure to marine environments.

The steel in concrete is in a passive state due to high pH (from 12 to 13). However, chloride ions and/or CO_2 may penetrate concrete through the pores and reach the interface steel concrete leading to local depassivation and, consequently, contributing to reduce the lifetime of many civil engineering structures.

Electrochemical techniques have proved to be useful tools to evaluate the corrosion resistance of metallic materials in laboratory and in the field [8, 9]. They allow short-term tests, the results of which enable extrapolations for longer periods. Cyclic voltammetry allows the identification of the various oxidation/reduction processes that

occur at the electrode/solution interface during the cyclic polarisation. It also allows testing the applicability of models, i.e., the model of the breakdown of passivity, known as the Point Defect Model (PDM) established by MacDonald et al. [10–13].

Several authors [14–26] have carried out cyclic voltammetric studies on iron and steel passivity in sodium and potassium alkaline media. The number of peaks shown on the recorded voltammograms is quite diverse. Joiret et al. [18] obtained six anodic peaks on a cyclic voltammogram of Fe in 1 M NaOH, recorded at 0.5 mV s^{-1}. On the contrary, in a study of AISI 304L in alkaline chloride medium (0.1 M NaOH + 0.5 M NaCl), Abreu et al. [21] observed only one anodic and the corresponding cathodic peak for polarisations in the Fe active potential region. Freire et al. [17] studied the behaviour of stainless steel in alkaline media (0.1 M NaOH) for polarisations between −1.4 and +0.6 V versus SCE at 1 mV s^{-1}. They obtained a single well-defined anodic peak in the iron active region, and a small oxidation peak in the transpassive region, which was attributed to the oxidation of Cr(0) to Cr(III).

Literature concludes that the nature and the amounts of anions can bring significant changes in the voltammetric profiles of iron and steel electrodes in alkaline media. Also small changes in pH, particularly in the range of 12–13, can contribute to the appearance of peaks in the transpassive region which have been attributed to the oxidation of Fe(III) to Fe(VI) [19, 20].

Concerning the electrochemical behaviour of steel in $Ca(OH)_2$ aqueous solutions, only a few studies have been published [14, 15, 22–26]. As reported by Albani et al. [14, 15] and more recently by Hinatsu et al. [22], the nature of the cation (Na^+, K^+ or Ca^{2+}) can strongly contribute to induce changes on the cyclic voltammetric profiles. Small differences in the pH values in alkaline media can also bring differences in Fe and steel electrochemical behaviour. In $Ca(OH)_2$ aqueous solutions, no data evaluating the effects of chloride ions in terms of the corrosion kinetic parameters seem to have been previously published.

The present study reports a systematic voltammetric study of prestressed steel immersed in saturated $Ca(OH)_2$ aqueous solution, in the absence and in the presence of 0.05 M and 0.5 M chloride ions, the latter simulating seawater composition. In order to verify the applicability of the Point Defect Model (PDM) to the breakdown of the passivity of steel in saturated $Ca(OH)_2$ containing 0. 5 M NaCl, cyclic voltammograms have been recorded in a wide range of scan rates (0.010–0.300 V s^{-1}).

Quasi-steady state polarisation curves, covering a wide range of polarisation potentials (from H_2 to O_2 evolution), have been recorded at 0.1 mV s^{-1}. The section corresponding to the active corrosion has been analysed by the linear polarisation resistance (LPR) method and the Tafel plots analysis.

2 Experimental

The composition of the pressurised steel used in this study is given in Table 1. Discs of prestressed steel (area: 0.07 cm^2) were soldered to a copper wire and then inserted into glass tubes. The contacts were insulated with Araldite. The electrodes were successively polished using SiC paper (grain sizes: no. 280, 600, 800 and 1,000), and Al_2O_3 (ALPHA Micropolish II, agglomerated, Buehler) of different grain sizes, 1, 0.3 and 0.05 μm. A platinum grid counter electrode and a commercial Ag/AgCl (KCl saturated) reference electrode completed the configuration of a three-electrode cell.

A saturated solution of $Ca(OH)_2$ was prepared using Milli pore Milli-Q water at boiling temperature. It was then left to cool and filtered. Saturated solutions of $Ca(OH)_2$ containing 0.5 mol L^{-1} NaCl were also prepared. Prior to electrochemical experiments, all solutions have been deoxygenated by oxygen-free N_2 bubbling for about 20 min; N_2—U Quality from L′Air Liquide was employed. In order to prevent the entrance of CO_2 into the system, the pH was checked from time to time using a portable pH meter from Radiometer Analytical.

Cyclic voltammetry and linear sweep voltammetry were performed through AUTOLAB® PGSTAT12/General Purpose Electrochemical System (GPES) from Eco Chemie B.V. All experiments were conducted keeping the electrochemical cell inside a Faraday cage. Linear polarisation resistance, R_p, was obtained from the analysis of the polarisation curves recorded at 0.1 mV s^{-1} (linear fitting ± 10 mV around $E(i = 0)$), while the corrosion current densities and corrosion potentials were obtained from the intersection of the anodic and cathodic Tafel lines. From the slopes of Tafel lines the values of β_a and β_c were determined. The breakdown passivity potential, E_b, as well as the repassivation potential, E_{repass}, were obtained

Table 1 Chemical composition of the steel, in percentage (%)

C	Si	Mn	P	S	Mo	Cr	Ni	Cu	V	N	Fe
0.90	0.19	0.81	0.02	0.007	0.005	0.25	0.023	0.015	0.003	0.04	Bal.

following the methodology described by MacDonald et al. [10].

SEM studies were performed using a scanning electron microscope (JEOL, model JSM-6400). The EDS spectra were recorded with an INCA X-ray microanalysis system (Oxford Instruments).

3 Results and discussion

3.1 Voltammetric study

3.1.1 Successive cycles

Figure 1 presents cyclic voltammograms (CVs) corresponding to successive polarisation cycles running between −1.2 and +0.50 V versus Ag/AgCl, at 0.1 V s^{-1}. Differences between the successive runs are observed particularly on the anodic peak definition and intensity. From the second run onwards, a well-defined pair of peaks, A_1/C_1, was recorded. It appears at −0.60 and −1.0 V versus Ag/AgCl, respectively. From the second to the third run the current densities doubled, but then they tend to be constant. After the first oxidation peak, the current density decreases to ca 400 μA cm^{-2} and at least until +0.5 V the passive region is observed. Albani et al. [14, 15] observed a similar behaviour for Fe in different alkaline solutions. They concluded that there are no effects of chloride ions in the corrosion active region. Hinatsu et al. [22] found a peak identical to peak A_1, at 0.6 V versus Ag/AgCl, on the voltammetric study of Fe in cement. They assigned it to ferrous–ferric transformations such as,

$$Fe(OH)_2 + OH^- \rightarrow \delta\text{-}FeOOH + H_2O + e^- \quad (1)$$

As shown in Fig. 2, the magnitude of peak C_1 increases when the potential is held in the passive region. Although the anodic peak is not expected to increase, an enhancement occurs. This may be the result of an increase in the reactivity of the steel surface after each run.

Peak current densities and consequently the corresponding charges vary with the holding time, but only for short periods (≤ 10 min). From then on, peak C_1 remains at an almost constant charge of 5 mC cm^{-2} (see data in Table 2).

3.1.2 Sweep rate study

Figure 3 provides a set of CVs for steel in saturated $Ca(OH)_2$ aqueous solutions polarised between −1.2 and 0.05 V, at various sweep rates applied in a descending order.

Plots of log I_p versus log v, for peaks A_1 and C_1, produce good straight lines with a slope of 0.5, while peak potentials do not present significant variations. The sweep rate dependence of peaks A_1 and C_1 is consistent with that predicted from the layer pore resistance model (LPRM) [27].

Figure 4 presents a set of CVs of steel electrodes in a saturated $Ca(OH)_2$ aqueous solution and in a saturated $Ca(OH)_2$ + 0.5 M NaCl solution, with the anodic polarisation potential limit, $E_{\lambda a}$, increasing successively. Data in Fig. 4a, c show CVs due to polarisations with an anodic limit, $E_{\lambda a}$, in the passive region, while CVs of Fig. 4b, d reveal polarisations reaching the transpassive region. In the absence of chloride ions, peak A_1 and its counter part, peak C_1, appear at −0.60 and −0.96 V versus Ag/AgCl, respectively, with a peak separation of the order of 360 mV, and a small oxidation peak (peak A_2) in the passive region at ca −0.2 V. In the presence of chloride ions, at 0.1 V s^{-1}, peak A_1 almost disappears; the passive region is strongly reduced, and under particular conditions, an anodic peak was observed in the transpassive region (see Fig. 4d).

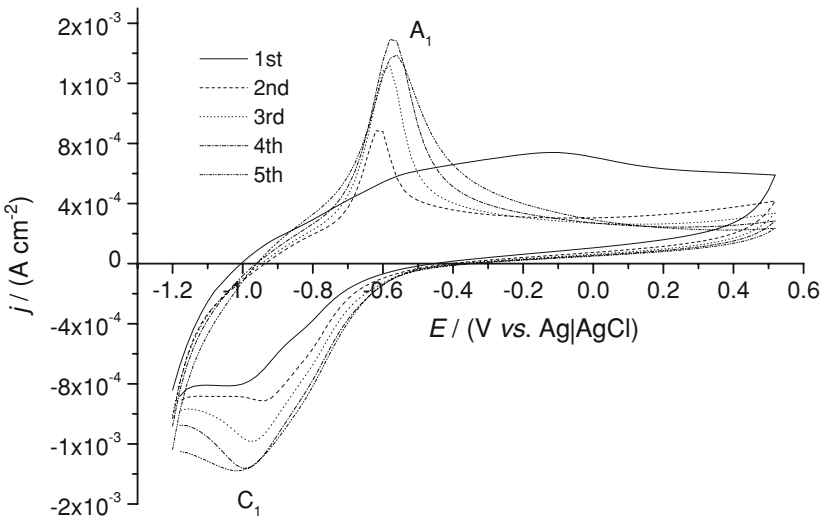

Fig. 1 Successive cyclic voltammograms of steel in saturated $Ca(OH)_2$ aqueous solution. $E_i = -1.2$ V; $E_{\lambda a} = +0.50$ V versus Ag/AgCl; $v = 0.1$ V s^{-1}

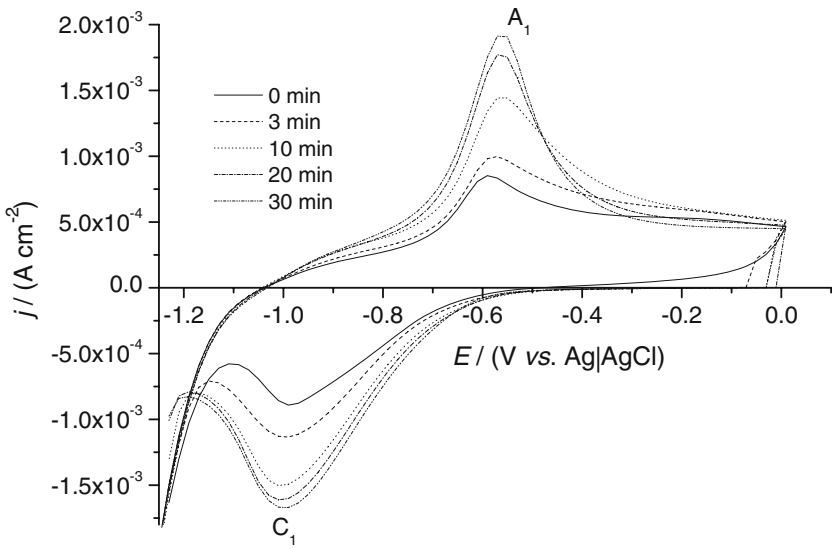

Fig. 2 Effects of holding the polarisation potential of the prestressed steel electrode in the passive region: **a** steel in saturated $Ca(OH)_2$. $E_i = -1.2$ V; $E_{\lambda a} = 0.0$ V; $v = 0.1$ V s^{-1}; $n = 2$

Table 2 Charge density of peak C_1 as a function of the holding time, at 0.0 V versus Ag/AgCl

t (min)	0	3	10	20	30
Q_p^{C1} (μC cm^{-2})	2,670	3,870	4,993	5,125	5,311

According to the literature [14, 15, 17–19, 21, 23, 24], peak A_1 is related to the oxidation of Fe(II) to Fe(III) and subsequent reaction with hydroxyl ions leading to iron oxides/hydroxides.

Sánchez et al. [23, 24] concluded that $Fe(OH)_2$ is formed by the oxidation of Fe, at cathodic potentials over −0.5 V versus Ag/AgCl, and by reactions with hydroxide species leading to the formation of Fe(III) oxides according to the following equations:

$$3Fe(OH)_2 + 2OH^- \rightarrow Fe_3O_4 + 4H_2O + 2e^- \quad (2)$$

$$3Fe_3O_4 + 2OH^- \rightarrow 3\gamma\text{-}Fe_2O_3 + H_2O + 2e^- \quad (3)$$

and/or

$$Fe_3O_4 + OH^- \rightarrow 3\alpha\text{-}FeOOH + e^- \quad (4)$$

It is stated in the literature [24] that the passive layer is composed by an inner layer, formed at about −0.8 V versus SCE, and an outer layer, composed by γ-Fe_2O_3 and α-FeOOH.

For polarisations in the transpassive region in the absence of chloride, peaks A_1 and C_1 increase in size as $E_{\lambda a}$ becomes more anodic. As the potential becomes more positive than 0.8 V, the current rises abruptly and the transpassive dissolution of Fe occurs simultaneously with O_2 evolution.

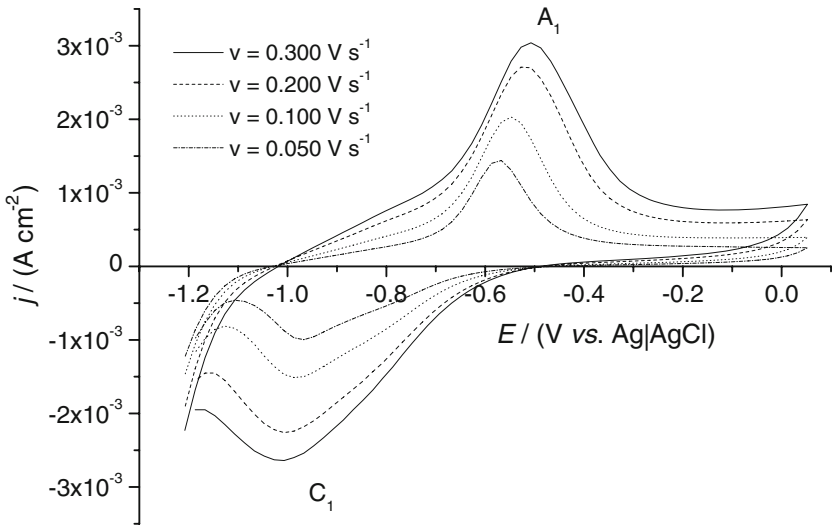

Fig. 3 CVs of prestressed steel in saturated $Ca(OH)_2$ as a function of sweep rate

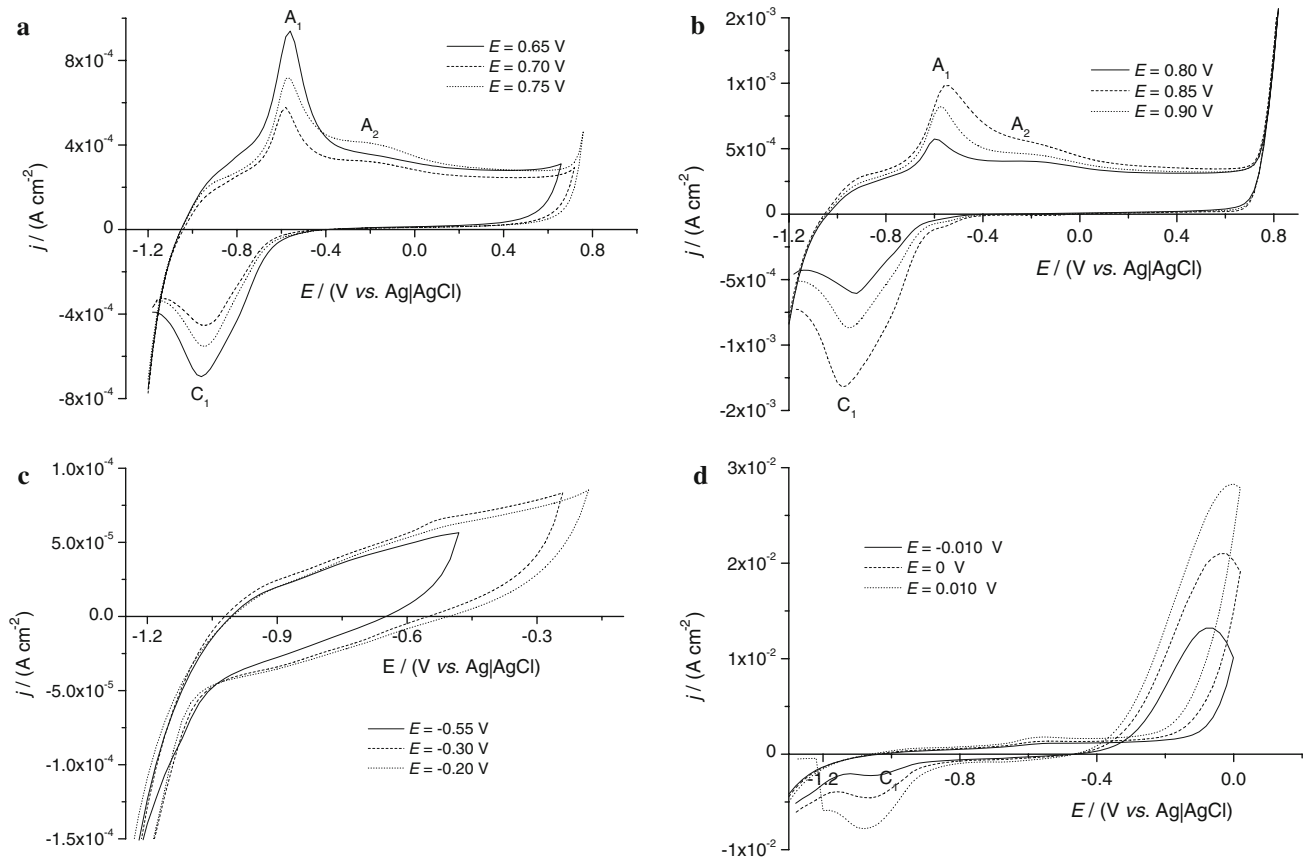

Fig. 4 CVs of prestressed steel as a function of the anodic polarisation potential, $E_{\lambda a}$: **a** and **b** in saturated $Ca(OH)_2$ aqueous solution; **c** and **d** in saturated $Ca(OH)_2$ + 0.5 M NaCl. $E_i = -1.15$ V, $v = 0.1$ V s^{-1}; $n = 2$

In the presence of 0.5 M chloride ions, for $E_{\lambda a}$ values in the passive region, peak A_1 is not well defined, while peak C_1 is observed at ca −1.1 V and increases in size as the polarisation potential reaches the transpassive region, such as for $E_{\lambda a} \geq -0.010$ V. Small increments of potential then lead to the crossover of the anodic currents defining a repassivation potential. Voltammetric studies of Fe or steel in alkaline media have demonstrated a similar behaviour [18, 21].

CVs of steel/$Ca(OH)_2$ and steel/$Ca(OH)_2$ + 0.5 M NaCl interfaces recorded under identical experimental conditions are presented in Fig. 5, for comparison purposes. These CVs clearly show the drastic effect of chloride in terms of the breakdown potential, E_b, which is displaced negatively by ca 1.0 V for 0.5 M chloride concentration (see data in Table 3). Another important feature is the crossover of the anodic currents. A repassivation potential, E_{repass}, can be obtained from the analysis of the CVs presented in Fig. 5.

Data in Table 3 show also that as the chloride ions concentration increases the breakdown potential is displaced to less positive potentials and both the extension of the passivation region and the overpotential of repassivation are drastically reduced. For the higher chloride

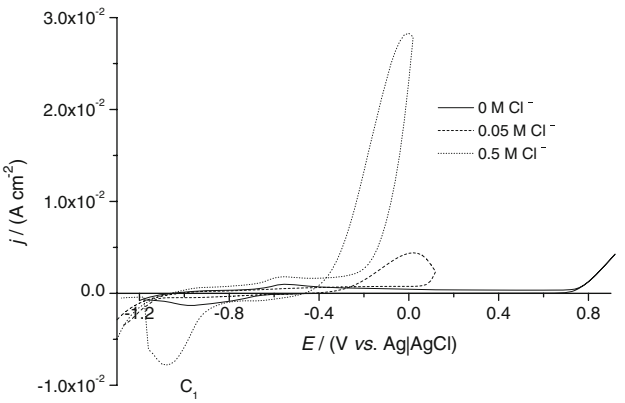

Fig. 5 CVs of prestressed steel in saturated $Ca(OH)_2$ aqueous solution in the absence and presence of 0.5 M of NaCl. $v = 0.1$ V s^{-1}, $n = 2$

concentration (0.5 M), the extension of the passive region is reduced from ca 1.7 to 0.6 V. The breakdown of passivity is strongly influenced by the chloride concentration. The crossover of two anodic currents is indicative of the nucleation processes [28, 29], and according to the literature, during the breakdown of passive films, nucleus is

Table 3 Electrochemical parameters from the analysis of the CVs of steel in saturated $Ca(OH)_2$ + *x* M NaCl

[NaCl] *M*	$E_{\lambda a}$	E_b	E_{repass}	ΔE_{pass}	η_{repass}	$E_p(A_1)$	$E_p(C_1)$
	V versus Ag/AgCl			mV		V versus Ag/AgCl	
0	+0.900	+0.800	+0.730	1,720	70	−0.60	−0.97
0.05	+0.100	+0.060	−0.260	1,080	320	–	–
0.5	+0.040	−0.234	−0.388	611	154	–	−1.05

$v = 0.1$ V s^{-1}, $n = 2$

found where pitting is to be initiated. Under certain conditions, these pits are susceptible to reactivate, but at more aggressive conditions they do not repassivate and, most certainly, generalised corrosion will occur.

3.1.3 The transpassive region

Cyclic voltammetry of steel in saturated $Ca(OH)_2$ solution containing 0.5 M NaCl was carried out with polarisations covering the transpassive region, at sweep rates ranging from 0.3 to 0.02 V s^{-1}. The CVs recorded at 0.2 and 0.05 V s^{-1} are presented in Fig. 6a. The breakdown potential, E_b, as a function of the square root of the sweep rate, $v^{1/2}$, is plotted in Fig. 6b.

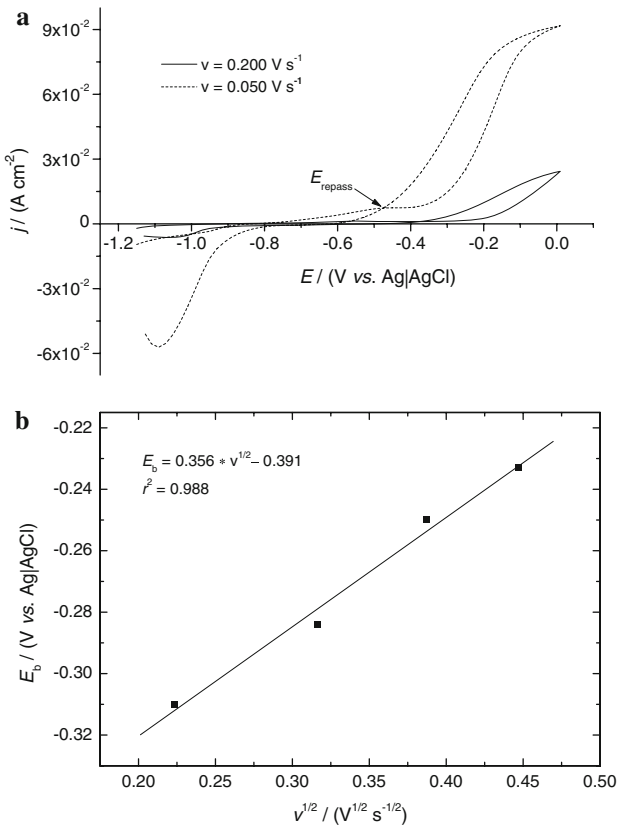

Fig. 6 **a** CVs of steel in saturated $Ca(OH)_2$ + 0.5 M NaCl as a function of the scan rate. $E_i = -1.1$ V; $E_{\lambda a} = 0.0$ V; **b** Plots of E_b versus $v^{1/2}$

Table 4 Repassivation potentials and overpotentials as function of the sweep rate (*v*)

v (V s^{-1})	E_{repass} V versus Ag/AgCl	η_{repass} mV
0.300	−0.273	57
0.200	−0.383	126
0.050	−0.477	167
0.020	−0.544	182

CVs clearly show the displacement of the breakdown potential, E_b, and of the repassivation potential, E_{repass}, to less anodic potential values, as the scan rate decreases (see data in Table 4).

As expected, the overpotential for the repassivation increases as the sweep rate decreases. In fact, longer polarisations must lead to pits of higher size, consequently, of more difficult repassivation. A plot of the breakdown potentials, E_b, as a function of the square root of the scan rate is in agreement with the point defect model (PDM) of MacDonald [11]. The slope of the straight line presents a value of 0.35 $(Vs)^{1/2}$ identical to the value obtained in a previous study of Al2024 in seawater solution [30].

3.2 Quasi-steady state polarisation curves

In order to obtain the corrosion parameters, R_p, E_{corr} and j_{corr}, the linear polarisation curves were recorded at 0.1 mV s^{-1}, they are displayed in Fig. 7a, b. Their analysis through the polarisation resistance method gives R_p values, and the Tafel analysis gives the values of E_{corr}, j_{corr} and Tafel slopes (see data in Table 5).

Values of the Tafel slopes are indicative of a kinetic controlled electron transfer process. The Tafel slope of the cathodic reaction ranges from 0.101 to 0.136 V dec^{-1}. Zhou [31] obtained similar values from the study of Fe in sodium alkaline solutions. This result is consistent with the following mechanism for the hydrogen evolution:

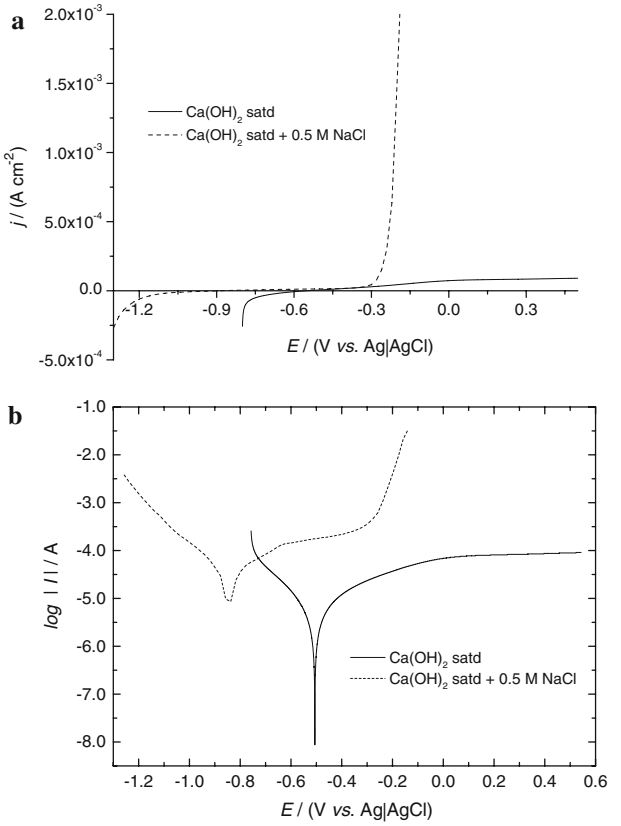

Fig. 7 **a** Polarisation curves of steel/saturated $Ca(OH)_2$ and steel/saturated $Ca(OH)_2$ + 0.5 M NaCl interfaces. $v = 0.1$ mV s^{-1}; **b** log $|I|$ versus E plots

$$H_2O + e^- \rightarrow H_{ads} + OH^- \quad (5)$$

$$H_{ads} + H_{ads} \rightarrow H_2 \quad (6)$$

where Eq. 5 is the rate determining step. As expected, the values of R_p decrease as the chloride ion concentration increases. According to the literature, values of R_p lower than 1×10^3 Ω cm^2 relate to active corrosion.

The polarisation resistance and consequently the corrosion current density values change by a factor in the order of ten due to the presence of chloride ions (0.5 M). The corrosion potential is displaced to the negative direction as the chloride concentration increases.

3.3 Open circuit potential experiments

3.3.1 Open circuit potential curves

Figure 8 presents the E_{OCP} curves of a two-week immersion of steel in saturated $Ca(OH)_2$ aqueous solution in the absence and in the presence of chloride ions. The curve corresponding to the immersion in the presence of chloride ions shows much more negative values for the open circuit potentials. This behaviour is in accordance with what is expected from a more aggressive environment. On the other hand, the curve corresponding to the behaviour in saturated $Ca(OH)_2$ aqueous solution starts with a value of −0.55 V and abruptly increases to an almost constant value of ca −0.25 V versus Ag/AgCl. This behaviour is characteristic of the passive state. In the presence of chloride, the initial value of the OCP is close to −0.33 V, decreases abruptly and in 2 days reaches the value of −0.45 V, then passes through a maximum at −0.40 V and thereafter, during the next 6 days, decreases slowly to −0.47 V. This behaviour can in principle be attributed to the formation of active sites, most probably pits as shown in the SEM micrographs (see Fig. 9).

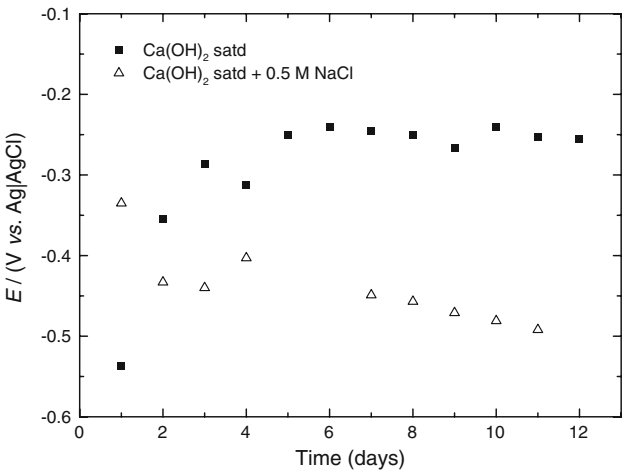

Fig. 8 Open circuit potential curves of steel immersed in $Ca(OH)_2$ saturated and in $Ca(OH)_2$ saturated + 0.5 M NaCl

Table 5 Electrochemical corrosion parameters from the Linear Polarisation Resistance (LPR) and Tafel analysis

[NaCl] M	*LPR*			Tafel analysis	
	R_p (Ω cm^2)	β_a mV dec^{-1}	β_c mV dec^{-1}	E_{corr} V versus Ag/AgCl	j_{corr} (μA cm^{-2})
0	8.0×10^3	0.087	0.132	−0.514	2.0
0.05	4.5×10^3	0.049	0.101	−0.692	3.2
0.50	0.9×10^3	0.050	0.136	−0.827	19.0

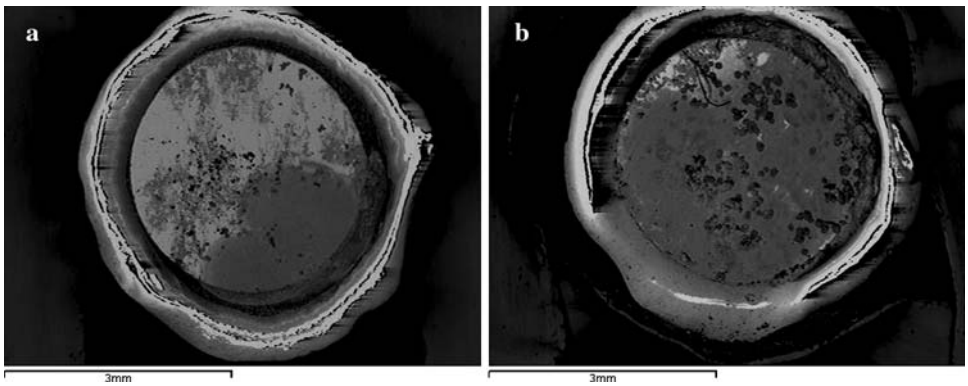

Fig. 9 SEM micrographs of the steel samples after two-week immersion in: **a** saturated $Ca(OH)_2$ + 0.05 M NaCl; **b** $Ca(OH)_2$ + 0.5 M NaCl secondary electrons (SE)

3.3.2 *Quantification of Fe in solution by atomic absorption spectroscopy*

Solutions from two-week steel immersions in saturated $Ca(OH)_2$ + 0.5 M NaCl and in saturated $Ca(OH)_2$ solutions have been analysed by atomic absorption spectroscopy; the results for iron concentration were 3.86 ppm and less than 1 ppm, respectively. The chemical analysis shows, as expected, that the dissolution of Fe in the saturated $Ca(OH)_2$ solution is almost null, while in the presence of chloride the Fe ions concentration in solution is close to 4 ppm.

3.4 SEM/EDS studies

The SEM micrographs of the steel samples from two-week immersion in the saturated $Ca(OH)_2$ aqueous solution containing chloride ions (Fig. 9a, b) show very differentiated morphologies with white (metallic), grey and black zones. The white zones predominate on the samples immersed in the solution with less amounts of chloride ions (0.05 M). No white zones are observed on the SEM images of the steel sample from immersions in saturated $Ca(OH)_2$ + 0.5 M NaCl.

The elemental analysis of the spectra corresponding to the white, grey and black coloured zones on the SEM images of Fig. 9 is shown in Table 6. The white (metallic) zones are most probably non-attacked zones, since they present a composition similar to the alloy as received, while the black zones are related to the presence of corrosion products, probably iron and calcium oxides/hydroxides, calcium carbonate and some iron or calcium chlorides and/or carbonates. Iron chlorides could predominate in solutions of high chloride ion concentration.

Since the composition of the passive film is quite well established in the literature, the present work does not address that purpose.

Table 6 Elemental composition of the corrosion products in (w/w)

Figure	Colour	Fe	C	O	Ca	Mn	Si	K	S	Cl	Cr	Na
9a	White	95	3	–	–	0.8	0.4	–	–	–	0.2	–
	Grey	45	14	37	2	0.8	0.4	0.8	0.07	–	0.2	0.8
	Black	14	60	16	6	0.9	0.4	1	0.07	–	0.2	1.0
9b	Grey	33	16	45	–	0.8	0.3	–	–	5	0.2	0.8
	Black	48	2.6	44	–	0.9	0.2	–		5	0.2	
	Alloy	98	0.9	–	–	0.8	0.2	–	–	–	0.2	–

4 Conclusions

Cyclic voltammograms of prestressed steel in saturated $Ca(OH)_2$ aqueous solutions have revealed a pair of conjugated peaks (A_1/C_1) in the iron active region, at −0.60 and −1.0 V versus Ag/AgCl, respectively. These peaks are due to the oxidation/reduction of Fe(II)/Fe(III). The peak current densities increased with the scan rate and continuous cycling.

At sweep rates ranging from 0.3 to 0.02 V s^{-1}, peak currents of peaks A_1 and C_1 have shown to be proportional to the square root of the scan rate, according to the pore growth model.

On the other hand, the CVs of steel samples polarised in saturated $Ca(OH)_2$ aqueous solution containing 0.5 M chloride ions show that peak A_1 becomes ill-defined in the iron active region, and the extension of the passive region is strongly reduced.

A linear dependence of the passivity breakdown potential, E_b, on the square root of the scan rate is obtained, following the PDM of MacDonald. A crossover characteristic of the nucleation processes (in this case nucleus for pitting to occur) is observed in the presence of chloride ions. As expected, polarisations at lower scan rates lead to high values of the repassivation overpotential.

In the presence of chloride ions, the corrosion current densities in the active region change from ca 2 to 20 μA cm^{-2}, while the polarisation resistance, R_p, decreases from 8.0×10^3 to 0.9×10^3 Ω cm^2 and the corrosion potential is displaced from −0.50 to −0.80 V

versus Ag/AgCl. These data show that chloride influences not only the passive and transpassive regions but also the active corrosion region.

The SEM/EDS studies revealed, as expected, a large amount of corrosion products on the samples immersed in the solution containing higher amounts of chloride ions. The surface morphology is also significantly affected by the chloride ion contents.

Since, significant differences were observed in the presence of chloride ions (0.5 M) in the passive and transpassive regions and in the active region, we can conclude that chloride ions contribute to enhance the kinetics of corrosion of passivated steel, most probably due to adsorption on both the active and the passive electrode surface.

Acknowledgements The authors acknowledge the financial support of FCT and FEDER through the programme POCI 2010 (Projects POCI/ECM/55692/2004 and PPCD/ECM/55692/2004). FCT is also acknowledged for the financial support to Centro de Ciências Moleculares e Materiais (CCMM) and Unidade de Química Ambiental [528].

References

1. Masullo A, Nunziata S. http://www.studionunziata.com/. Accessed 5 Nov 2008
2. Salas RM, Schokker AJ, West JS, Breen JE, Kreger M (2002) Mater Corros 53:591
3. Wilkins JM, Lawrence PF (1983) In: Crane AP (ed) Fundamental mechanism of corrosion of steel. Ellis Horwood, Chichester, UK
4. Sørenson P, Jensen B, Maahn E (1990) In: Page CL, Treadaway KWJ, Bamforth PB (eds) Corrosion of reinforcement in concrete. Elsevier Applied Science, London
5. Scully JR, Scully HS (1993) Corros J 49:99
6. Leeming MB (1983) In: Crane AP (ed) Corrosion of reinforcement in concrete construction. Society of Chemical Industry, London
7. Page CL, Treadaway KW (1975) Lett Nat 258:514
8. Kelly RG, Scully JR, Shoesmith DW, Buchheit RG (2003) Electrochemical techniques in corrosion science and engineering. Marcel Dekker, New York
9. Fonseca ITE (1987) Corros Prot Mater 6:37
10. Lei K-S, MacDonal DD, Pound BG, Wilde BE (1988) J Electrochem Soc 135:1625
11. Haruna T, MacDonald DD (1997) J Electrochem Soc 144:1574
12. MacDonald DD (1992) J Electrochem Soc 139:3434
13. Lin LF, Chao CY, MacDonald DD (1981) J Electrochem Soc 128:1194
14. Albani OA, Gassa LM, Zerbino JO, Vilche JR, Arvia AJ (1990) Electrochim Acta 35:1437
15. Albani OA, Gassa LM, Zerbino JO, Vilche JR, Arvia AJ (1986) Electrochim Acta 31:1403
16. Juanto S, Zerbino JO, Miguez MI, Vilche JR, Arvia AJ (1987) Electrochim Acta 32:1743
17. Freire L, Nóvoa XR, Pena G, Vivier V (2008) Corros Sci 50:3205
18. Joiret S, Keddam M, Nóvoa XR, Pérez MC, Rangel C, Takenouti H (2002) Cem Concr Compos 24:7
19. Rangel CM, Leitão RA, Fonseca ITE (1989) Electrochim Acta 34:55
20. Rangel CM, Leitão RA, Fonseca ITE (1986) Electrochim Acta 31:1659
21. Abreu CM, Cristóbal MJ, Losada R, Nóvoa XR, Pena G (2006) Electrochim Acta 51:1881
22. Hinatsu JT, Graydon WF, Foulks FR (1988) J Appl Electrochem 19:868
23. Sánchez M, Gegori J, Alonso MC, Garcia-Jareño JJ, Vicente V (2006) Electrochim Acta 52:47
24. Sánchez M, Gegori J, Alonso MC, Garcia-Jareño JJ, Takenouti H, Vicente V (2007) Electrochim Acta 52:7634
25. Addari D, Elsener B, Rossi A (2008) Electrochim Acta 53:8078
26. García-Alonso M, Escudero ML, Miranda JM, Vega MI, Capilla F, Correia MJ, Salta M, Bennani A, González JA (2007) Cem Concr Res 37:1463
27. Devilliers D, Lantelme F, Chemla M (1986) Electrochim Acta 31:1235
28. Chialvo MRG, Salvarezza RC, Moll DV, Arvia AJ (1985) Electrochim Acta 30:1501
29. Southampton Electrochemistry Group (1985) Instrumental methods in electrochemistry. Ellis Horwood Ltd, Chichester, UK
30. Fonseca ITE, Lima N, Rodrigues JA, Pereira MIS, Salvador JCS, Ferreira MGS (2002) Electrochem Commun 4:353
31. Zhou JY, Chin D-T (1987) Electrochim Acta 32:1751